

EFFECT OF CHEMICAL REACTION AND VISCOUS DISSIPATION ON MHD NANOFUID FLOW OVER A HORIZONTAL CYLINDER: ANALYTICAL SOLUTION

Nisha Shukla¹, Puneet Rana^{1*}, O. Anwar Béğ² and Bani Singh¹

¹*Department of Mathematics, JIIT Noida, Uttar Pradesh, India.*

²*Fluid Mechanics and Nanosystems, Aeronautical/Mechanical Engineering, Salford University, England, UK*

*Corresponding and presenting author : Email: puneetranaiitr@gmail.com, puneet.rana@jiit.ac.in

Abstract: An analytical study of the MHD boundary layer flow of electrically conducting nanofluid over a horizontal cylinder with the effects of chemical reaction and viscous dissipation is presented. Similarity transformations have been applied to transform the cylindrical form of the governing equations into the system of coupled ordinary differential equations and then homotopy analysis method has been implemented to solve the system. HAM does not contain any small or large parameter like perturbation technique and also provides an easiest approach to ensure the convergence of the series of solution. The effects of chemical reaction parameter, magnetic parameter and other important governing parameters with no flux nanoparticles concentration is carried out to describe important physical quantities.

Keywords: Homotopy analysis method; Nanofluid; MHD; Chemical reaction; Stretching cylinder;

Nomenclature			
q_w	Wall heat flux (W)	v, u	Velocity components along x -axis and radial direction (m/s)
K	Chemical reaction coefficient (s^{-1})	T_∞	Ambient temperature (K)
T_w	Nanofluid temperature at surface (K)	T	Nanofluid temperature (K)
$Nb = \frac{\tau}{\alpha} D_B C_\infty$	Brownian motion parameter	$Nt = \tau \frac{D_T}{\alpha T_\infty} (T_w - T_\infty)$	Thermophoresis parameter
$Ec = \frac{V_w^2}{c_f (T_w - T_\infty)}$	Eckert number	$Pr = \frac{\nu}{\alpha}$	Prandtl number
G	Dimensionless stream function	$Re = \frac{V_0 x^2}{\nu}$	Reynolds number

$M = \sqrt{\frac{\sigma B_0^2}{V_0 \rho}}$	Dimensionless Magnetic field	$Sc = \frac{\nu}{D_B}$	Schmidt number
θ	Dimensionless temperature	ψ	Stream function
$\lambda = \frac{K\nu}{V_0 D_B}$	Chemical reaction parameter	η	Similarity variable
$\gamma = \sqrt{\frac{\nu}{r_0^2 V_0}}$	Curvature parameter	$\tau = \frac{(\rho c)_p}{(\rho c)_f}$	Ratio of heat capacities
S	Dimensionless nanoparticle concentration	α	Thermal diffusivity(m ² /s)
Subscript			
∞	Ambient condition	f	Fluid
w	Condition on surface	p	Nanoparticle

1. Introduction

The study of heat and mass transfer of nanofluid flow with effects of chemical reactions over the stretching surface has a wide range of applications in chemical industries like that production of polymers and food processing, evaporation, cooling and drying processes, nuclear reactors cooling and also in petroleum industries. The term nanofluid [1-3] represents a base fluid with suspension of metallic nanosized particles. The chemical reactions can change the property and quality of any product. Hence, many researchers are considering the effects of chemical reactions in different types of problems. Krishnamurthy *et al.*[4] have presented a numerical study of MHD boundary layer flow of Williamson nanofluid over a horizontally linear stretching sheet with chemical reaction and radiation effects. They observed that the concentration of nanoparticles in boundary layer is decreased with increase in the value of chemical reaction parameter. Mohamed [5] has carried out the effects of chemical reactions and absorption on a mixed convective boundary layer flow past an exponentially stretching sheet and obtained that Sherwood number is an increasing function of chemical reaction parameter. Venkateswarlu and Narayana [6] have provided the same study for the rotating system. Reddy *et al.*[7] have investigated the effects of chemical reaction and thermal radiation on an unsteady flow of nanofluid bounded by a moving vertical flat plate with convective and diffusive boundary conditions.

The present article deals with the analytical study of chemical reactive nanoparticles on flow and heat transfer over a horizontal stretching cylinder, which is not mentioned in any above literatures. We have applied homotopy analysis method [8-11] to solve the system of ordinary nonlinear differential equations which are the transformed form of governing equations.

2. Nanofluid Dynamic Model

In present problem, we analyze the effects of chemical reactions on a steady two dimensional boundary layer flow of an incompressible electrically conducting nanofluid past a horizontal stretching cylinder. The cylindrical coordinates (r, x) are taken along the radial and axial directions of cylinder, respectively and the stretching velocity of cylinder is $V_w = V_0 x$. A constant magnetic field B_0 is assumed to be applied in radial direction of cylinder [Fig.1]. The boundary layer equations, which represent such type of flow, can be written as [6, 12]:

$$\frac{u}{r} + \frac{\partial u}{\partial r} + \frac{\partial v}{\partial x} = 0, \tag{1}$$

$$\rho \left(u \frac{\partial u}{\partial r} + v \frac{\partial v}{\partial x} \right) = \mu \left(\frac{\partial^2 v}{\partial r^2} + \frac{1}{r} \frac{\partial v}{\partial r} \right) - \sigma B_0^2 v, \tag{2}$$

$$\left(u \frac{\partial T}{\partial r} + v \frac{\partial T}{\partial x} \right) = \frac{k}{(\rho c)_f} \left(\frac{\partial^2 T}{\partial r^2} + \frac{1}{r} \frac{\partial T}{\partial r} \right) + \frac{\mu}{(\rho c)_f} \left(\frac{\partial v}{\partial r} \right)^2 + \tau \left[D_B \frac{\partial T}{\partial r} \frac{\partial C}{\partial r} + \frac{D_T}{T_\infty} \left(\frac{\partial T}{\partial r} \right)^2 \right], \tag{3}$$

$$u \frac{\partial C}{\partial r} + v \frac{\partial C}{\partial x} = D_B \left(\frac{\partial^2 C}{\partial r^2} + \frac{1}{r} \frac{\partial C}{\partial r} \right) + \frac{D_T}{T_\infty} \left(\frac{\partial^2 T}{\partial r^2} + \frac{1}{r} \frac{\partial T}{\partial r} \right) - K(C - C_\infty). \tag{4}$$

The associated boundary conditions are:

$$v(x, r) = V_w, \quad u_w = 0, \quad T = T_w, \quad D_B \frac{\partial C}{\partial r} + \frac{D_T}{T_\infty} \frac{\partial T}{\partial r} = 0, \quad \text{at } r = r_0,$$

$$v(x, r) = 0, \quad T = T_\infty, \quad C = C_\infty, \quad \text{as } r \rightarrow \infty. \tag{5}$$

We introduce following similarity transformations to reduce the eqs. (2)-(5) into dimensionless form [12]:

$$\eta = \frac{r^2 - r_0^2}{2r_0} \sqrt{\frac{V_0}{\nu}}, \quad \psi = \sqrt{V_0 \nu} x r_0 G(\eta), \quad v = V_0 x G'(\eta), \quad u = -\frac{r_0}{r} \sqrt{V_0 \nu} G(\eta), \quad \theta = \frac{T - T_\infty}{T_w - T_\infty}, \quad S = \frac{C - C_\infty}{C_\infty}, \tag{6}$$

The non dimensional system of ordinary differential equations is

$$(1+2\eta\gamma)G''' + 2\gamma G'' - G'^2 + GG'' - M^2 G' = 0, \tag{7}$$

$$(1+2\eta\gamma)(\theta'' + Nb\theta'S' + Nt\theta'^2) + Pr[G\theta' + (1+2\eta\gamma)EcG'^2] + 2\gamma\theta' = 0, \tag{8}$$

$$(1+2\eta\gamma)\left[S'' + \frac{Nt}{Nb}\theta''\right] + 2\gamma\left[S' + \left(\frac{Nt}{Nb}\right)\theta'\right] + ScGS' - \lambda S = 0, \tag{9}$$

and transformed boundary conditions are

$$\begin{aligned} G(\eta) = 0, G'(\eta) = 1, \theta(\eta) = 1, NbS'(\eta) + Nt\theta'(\eta) = 0, & \quad \text{at } \eta = 0 \\ G'(\eta) = 0, \theta(\eta) = 0, S(\eta) = 0. & \quad \text{as } \eta \rightarrow \infty \end{aligned} \tag{10}$$

2.1. The physical quantities of interest

In this study, the important physical quantities are the measurement of coefficient of skin friction local Nusselt number and Sherwood number, which are defined as:

$$C_G = \frac{\tau_w}{\rho v_w^2}, \quad Nu_x = \frac{xq_w}{k(T_w - T_\infty)}, \quad Sh_x = \frac{xq_m}{D_B C_\infty}, \tag{11}$$

$$\text{where } \tau_w = \mu \left(\frac{\partial v}{\partial r}\right)_{r=r_0}, \quad q_w = -k \left(\frac{\partial T}{\partial r}\right)_{r=r_0} \quad \text{and} \quad q_m = -D_B \left(\frac{\partial C}{\partial r}\right)_{r=r_0}. \tag{12}$$

Applying similarity transformations (6) on the eqs. (11)-(14), we obtain

$$Re^{1/2} C_G = G''(0), \quad Re^{-1/2} Nu_x = -\theta'(0), \quad Re^{-1/2} Sh_x = -S'(0). \tag{13}$$

3. HAM Series Solution

To solve eqs. (7)-(10), we have selected following initial guesses, linear operators and auxiliary functions :

$$S_0(\eta) = 1 - \exp(-\eta), \quad \theta_0(\eta) = \exp(-\eta), \quad S_0(\eta) = -\frac{Nt}{Nb} \exp(-\eta), \tag{14}$$

$$L_G(G) = \frac{\partial^3 G}{\partial \eta^3} + \frac{\partial^2 G}{\partial \eta^2}, \quad L_\theta(\theta) = \frac{\partial^2 \theta}{\partial \eta^2} + \frac{\partial \theta}{\partial \eta}, \quad L_S(S) = \frac{\partial^2 S}{\partial \eta^2} + \frac{\partial S}{\partial \eta}, \quad H_G = H_\theta = H_S = 1.$$

3.1. The mth order deformation equations

$$L_G(G_m(\eta) - \chi_{m-1}G_{m-1}(\eta)) = h_G H_G R_m^G(\eta), \quad L_\theta(\theta_m(\eta) - \chi_{m-1}\theta_{m-1}(\eta)) = h_\theta H_\theta R_m^\theta(\eta),$$

$$L_S(S_m(\eta) - \chi_{m-1}S_{m-1}(\eta)) = h_S H_S R_m^S(\eta)$$

with boundary conditions: $G_m(0) = 0$, $G_m'(0) = 0$, $\theta_m(0) = 0$, $Nb S'(0) + Nt \theta'(0) = 0$,

$$\text{as } \eta \rightarrow \infty \quad G_m'(\eta) = 0, \quad \theta(\eta) = 0, \quad S_m(\eta) = 0, \quad (15)$$

where

$$R_m^G(\eta) = (1 + 2\eta\gamma)G_{m-1}''' + 2\gamma G_{m-1}'' + \sum_{i=0}^{m-1} (G_i G_{m-1-i}'' - G_i' G_{m-1-i}') - M^2 G_{m-1}',$$

$$R_m^\theta(\eta) = (1 + 2\eta\gamma)(\theta_{m-1}'' + \sum_{i=0}^{m-1} (Nb\theta_i'\phi_{m-1-i}' + Nt\theta_i'\theta_{m-1-i}')) + \Pr \left[(1 + 2\eta\gamma)Ec \sum_{i=0}^{m-1} G_i'' G_{m-1-i}'' + \sum_{i=0}^{m-1} G_i \theta_{m-1-i}' \right] + 2\gamma\theta_{m-1}',$$

$$R_m^S(\eta) = (1 + 2\eta\gamma) \left[S_{m-1}'' + \left(\frac{Nt}{Nb} \right) \theta_{m-1}'' \right] + 2\gamma [S_{m-1}' + \theta_{m-1}'] + Sc \sum_{i=0}^{m-1} G_i \theta_{m-1-i}' - \lambda S_{m-1}.$$

The m^{th} terms $G_m(\eta)$, $\theta_m(\eta)$ and $S_m(\eta)$ are obtained by the following equations:

$$G_m(\eta) = G_m^*(\eta) + C_1 + C_2\eta + C_3e^{-\eta}, \quad (16)$$

$$\theta_m(\eta) = \Theta_m^*(\eta) + C_4 + C_5e^{-\eta}, \quad (17)$$

$$S_m(\eta) = S_m^*(\eta) + C_6 + C_7e^{-\eta}, \quad (18)$$

where $C_i (i = 1 \dots 7)$ are the constants, which can be obtained by the boundary conditions (15) and

$G_m^*(\eta)$, $\Theta_m^*(\eta)$ and $S_m^*(\eta)$ are represents the particular integrals. Hence the HAM series solutions are obtained in following form of equations:

$$G(\eta, q) = G_0(\eta) + \sum_{m=1}^{\infty} G_m(\eta), \quad \theta(\eta, q) = \theta_0(\eta) + \sum_{m=1}^{\infty} \theta_m(\eta), \quad S(\eta, q) = S_0(\eta) + \sum_{m=1}^{\infty} S_m(\eta). \quad (19)$$

3.2. Convergence of HAM

The convergence of the eqs. (16)-(18) are dependent upon the auxiliary parameters h_G , h_θ and h_S [9].

To find out the adequate values of these parameters, we have sketched the h -curves with $G''(0)$, $\theta'(0)$ and $S'(0)$ for different values of magnetic parameter M at 15-th order of approximations which are displayed in **Fig. 2**. These figures indicate that the acceptable ranges of h_G , h_θ and h_S are $h_G = [-0.7 \ -0.1]$, $h_\theta = [-0.25 \ -0.005]$, $h_S = [-0.25 \ -0.005]$ and **Table-1** ensure that the series solutions (19) are convergent upto four places of decimal for $h_G = -0.35$, $h_\theta = -0.125$ and $h_S = -0.125$.

4. Discussion of Results

In this section, we examine the effects of governing parameters such as magnetic parameter M , curvature parameter γ , chemical reaction parameter λ and Eckert number Ec on velocity $G'(\eta)$, skin friction coefficient $G''(0)$, temperature $\theta(\eta)$, rate of heat transfer $\{-\theta'(0)\}$, concentration $S(\eta)$ and Sherwood number $\{-S'(0)\}$. The default values of parameters are taken as $Nt = 0.3$, $Nb = 0.1$, $Pr = 7$, $M = 0.5$, $Ec = 0.5$, $Sc = 10$, $\gamma = 0.1$, $\lambda = 0.5$. We have compared the HAM results with shooting results which are presented in **Table-2 & 3**. These **Tables** represent a good agreement among the both results. The influence of leading parameters on physical quantities is presented graphically. **Fig. 3** is sketched to examine the effect of M on $G'(\eta)$, $\theta(\eta)$ and $S(\eta)$, which shows that $G'(\eta)$ decreases with an increase the value of M but $\theta(\eta)$ and $S(\eta)$ are increasing function of M . It is due to the physical fact that as magnetic parameter increases, the effect of Lorentz forces also increases which can reduce the motion, but temperature of system and nanoparticles species are increased due to these forces. **Fig. 4(a,b)** illustrates the effects of λ and γ on $\{-\theta'(0)\}$ and $\{-S'(0)\}$ which indicates that $\{-\theta'(0)\}$ reduces for the increasing values of λ and γ but $\{-S'(0)\}$ increases with these parameters. The combined effects of M and γ on $G''(0)$ is presented in **Fig. 4c** which represents that $G''(0)$ decreases as both these parameters increases. It means that chemical reactions can reduces the transfer of heat in the system but increases the mass transfer. **Fig. 5** is plotted to inspect the effects of Eckert number and magnetic parameter M on $\{-\theta'(0)\}$ and $\{-S'(0)\}$. $\{-\theta'(0)\}$ decreases with an increase the value of Ec and M but $\{-S'(0)\}$ increases with these parameters.

5. Conclusions

This article presents an analytical study of the effects of chemical reaction and viscous dissipation on a MHD nanofluid flow over a horizontal stretching cylinder. It is conclude that $G'(\eta)$ and $S(\eta)$ are decreasing functions M whereas $\theta(\eta)$ increases with it. $G''(0)$ reduces with an increase the value of M and γ . $\{-\theta'(0)\}$ decreases for the increasing value of chemical reaction parameter λ but $\{-S'(0)\}$

shows an opposite behavior with this parameter. $\{-\theta'(0)\}$ reduces as Ec and M increase whereas $\{-S'(0)\}$ decreases with these parameters.

References

1. S.U.S. Choi, J.A. Eastman, Enhancing thermal conductivity of fluids with nanoparticles, *Materials Science* 231 (1995) 99-105.
2. R. Saidur, K.Y. Leong, H.A. Mohammad, Review on applications and challenges of nanofluids, *Renewable and Sustainable Energy Reviews*, 15 (2011) 1646–1668.
3. J. Buongiorno, Convective transport in nanofluids, *ASME Journal of Heat Transfer*, 128 (2006) 240–250.
4. M. R. Krishnamurthy, B. C. Prasannakumara, B. J. Gireesha, R. S. R. Gorla, Effect of chemical reaction on MHD boundary layer flow and melting heat transfer of Williamson nanofluid in porous medium, *Engineering Science and Technology an International Journal*, 2015.
5. R. E. Mohamed, Chemical reaction effect on MHD boundary-layer flow of two-phase nanofluid model over an exponentially stretching sheet with a heat generation, *Journal of Molecular Liquids*, 220 (2016) 718-725.
6. B. Venkateswarlu , P. V. S. Narayana, Chemical reaction and radiation absorption effects on the flow and heat transfer of a nanofluid in a rotating system, *Applied Nanoscience*, 5 (2015) 351-360.
7. J.V. R. Reddy, V. Sugunamma, N. Sandeep, C. Sulochana, Influence of chemical reaction, radiation and rotation on MHD nanofluid flow past a permeable flat plate in porous medium, *Journal of the Nigerian Mathematical Society*, 35 (2016) 48–65.
8. S. J. Liao, *Beyond Perturbation: Introduction to Homotopy Analysis Method*, Chapman & Hall/CRC Press, London/Boca Raton, (2003).
9. T. Hayat, M. Imtiaz, A. Alsaedi, Unsteady flow of nanofluid with double stratification and magnetohydrodynamics, *International Journal of Heat and Mass Transfer*, 92 (2016) 100-109.
10. T. Zubair, M. Usman, U. Ali, S. T. Mohyud-Din, Homotopy analysis method for system of partial differential equations, *International Journal of Modern Engineering Sciences*, 2 (2012) 67-79.

11. B. Raftari, F. Parvaneh, K. Vajravelu, Homotopy analysis of the magnetohydrodynamic flow and heat transfer of a second grade fluid in porous channel, *Energy*, 59(2014) 625-632.
12. R. Dhanai, P. Rana, L. Kumar, MHD mixed convection nanofluid flow and heat transfer over an inclined cylinder due to velocity and thermal slip effects: Buongiorno's model, *Powder Technology*, 288 (2016) 140–150.

Table-1 Order of convergence of HAM for the values of $G''(0)$, $\theta'(0)$ and $S(0)$ for the fixed values of parameters $Nt = Nb = 0.1$, $Sc = 10$, $Ec = 0.1$, $M = 0.1$, $Pr = 1$, $\gamma = 0.1$, $\lambda = 0.5$, $h_G = -0.35$, $h_\theta = -0.125$, $h_S = -0.125$.

Order	10	20	30	35	40	50
$-G''(0)$	1.0416	1.0418	1.0418	1.0418	1.0418	1.0418
$-\theta'(0)$	0.6223	0.5557	0.5465	0.5460	0.5460	0.5460
$-S(0)$	0.1580	0.1636	0.1676	0.1686	0.1686	0.1686

Table-2 Numerical Comparison of HAM and Shooting results of $G''(0)$ for the different values of M and γ .

γ	0.1			0.2		
M	0.1	0.2	0.3	0.1	0.2	0.3
HAM	1.0418	1.0571	1.0822	1.0782	1.0941	1.1198
Shooting	1.0418	1.0572	1.0823	1.0782	1.0941	1.1199

Table-3 Numerical Comparison of HAM and Shooting results of $\{-\theta'(0)\}$ and $\{-S'(0)\}$ for the different values of Ec and γ and fixed values of parameters $Nt = Nb = 0.1$, $Sc = 10$, $Pr = 1$, $M = 0.1$,

$\lambda = 0.5$.

γ	Ec	$\{-\theta'(0)\}$		$\{-S'(0)\}$	
		HAM	Shooting	HAM	Shooting
0.1	0.1	0.5460	0.5460	0.1686	0.1686
	0.2	0.5019	0.5018	0.1616	0.1623
	0.3	0.4577	0.4575	0.1552	0.1560
0.2	0.1	0.5715	0.5726	0.1781	0.1782
	0.2	0.5252	0.5261	0.1707	0.1718
	0.3	0.4788	0.4796	0.1641	0.1653

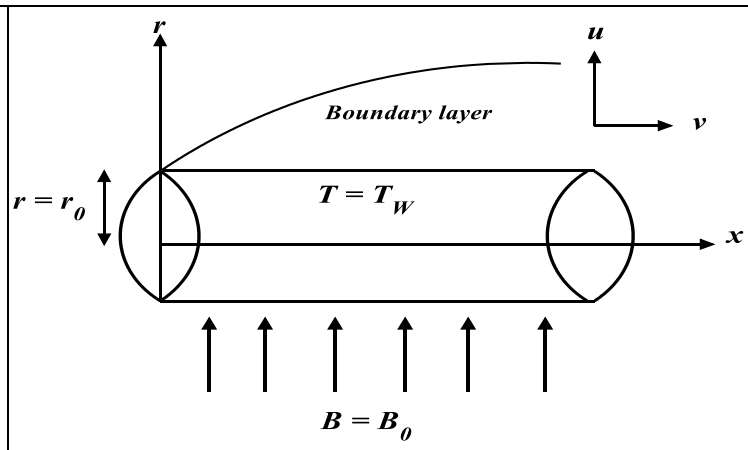


Figure 1. Physical Model with co-ordinate axes

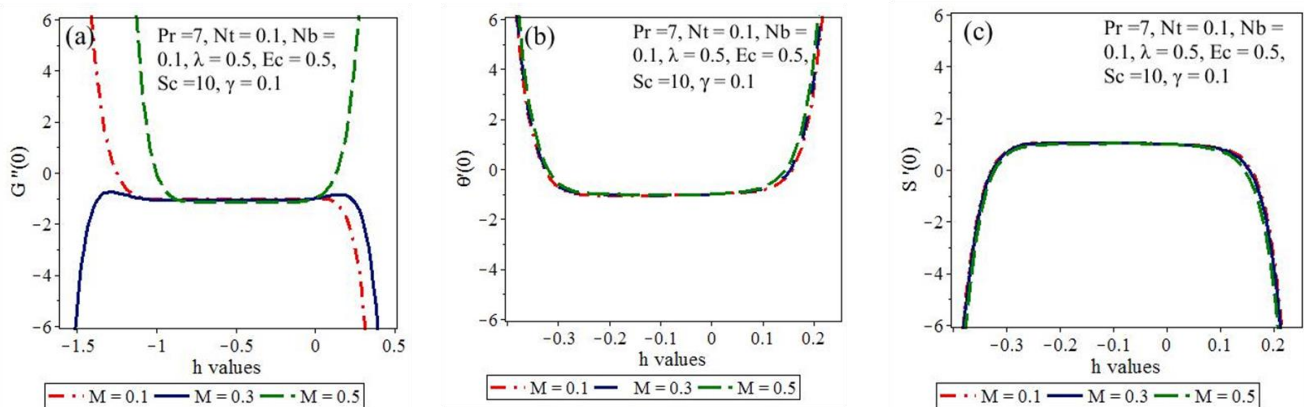


Figure 2. h-curves for dimensionless variables

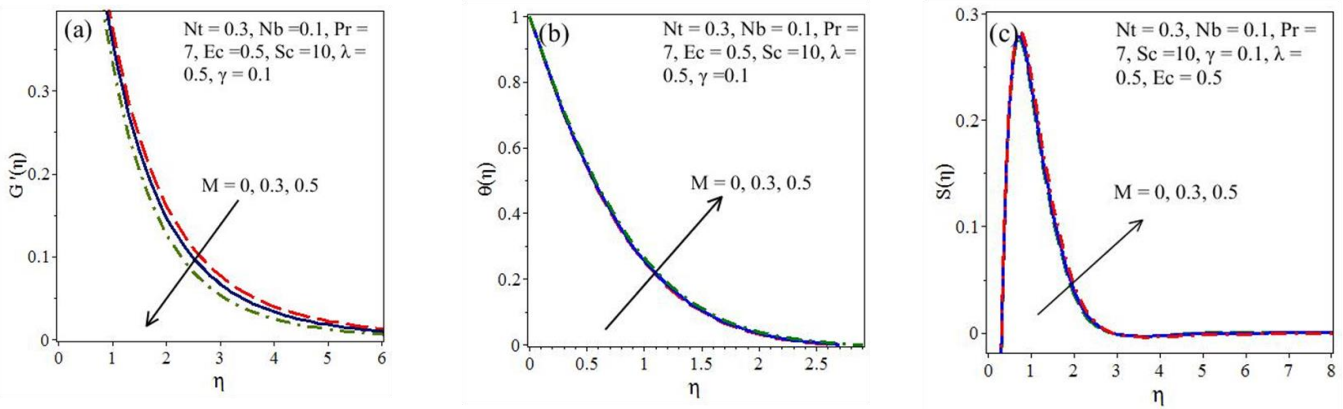


Figure 3. Effect of Magnetic field parameter on velocity, temperature and concentration profiles.

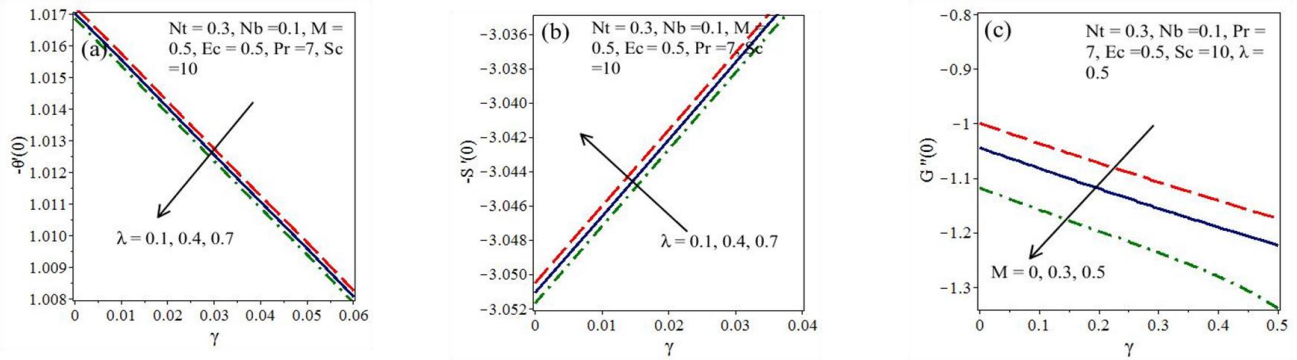


Figure 4. Effect of chemical reaction, curvature and magnetic field on heat and mass transfer.

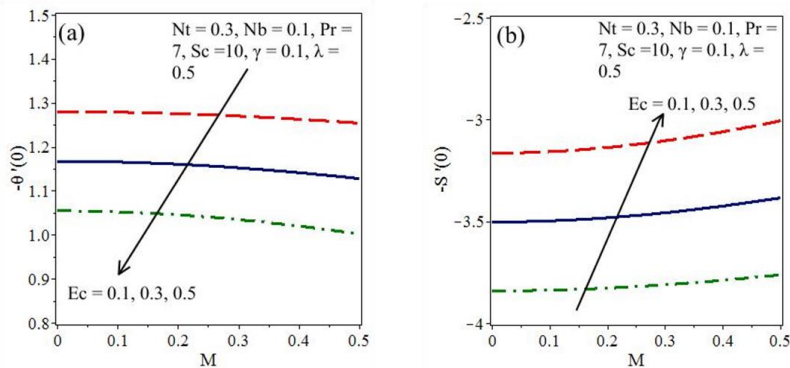


Figure 5. Combined effect of viscous dissipation and magnetic parameter on heat and mass transfer.